Test-beam results of a silicon pixel detector with Time-over-Threshold read-out having ultra-precise time resolution

2015 JINST 10 P12016

(http://iopscience.iop.org/1748-0221/10/12/P12016)

Published by IOP Publishing for Sissa Medialab

Received: *October 4, 2015*
Accepted: *December 3, 2015*
Published: *December 21, 2015*

Test-beam results of a silicon pixel detector with Time-over-Threshold read-out having ultra-precise time resolution

G. Aglieri Rinella,[a] **E. Cortina Gil,**[d] **M. Fiorini,**[a,b,1] **J. Kaplon,**[a] **A. Kluge,**[a] **F. Marchetto,**[c] **M. E. Martin Albarran,**[a] **M. Morel,**[a] **M. Noy,**[a] **L. Perktold,**[a] **S. Tiuraniem**[a] **and B. Velghe**[d]

[a] *CERN, CH-1211 Geneva 23, Switzerland*
[b] *INFN Sezione di Ferrara and Università degli Studi di Ferrara, Via Saragat 1, 44122 Ferrara, Italy*
[c] *INFN Sezione di Torino, Via Giuria 1, 10125 Torino, Italy*
[d] *Université Catholique de Louvain, Chemin du Cyclotron 2, B-1348 Louvain-la-Neuve, Belgium*

E-mail: Massimiliano.Fiorini@cern.ch

Abstract: A time-tagging hybrid silicon pixel detector developed for beam tracking in the NA62 experiment has been tested in a dedicated test-beam at CERN with 10 GeV/c hadrons. Measurements include time resolution, detection efficiency and charge sharing between pixels, as well as effects due to bias voltage variations. A time resolution of less than 150 ps has been measured with a 200 µm thick silicon sensor, using an on-pixel amplifier-discriminator and an end-of-column DLL-based time-to-digital converter.

Keywords: Particle tracking detectors; Timing detectors; Pixelated detectors and associated VLSI electronics

[1] Corresponding author.

doi:10.1088/1748-0221/10/12/P12016

2015 JINST 10 P12016

Contents

2015 JINST 10 P12016

1 The Gigatracker detector

A hybrid silicon pixel detector, named GigaTracKer (GTK), was developed for beam tracking in NA62, the experiment designed to detect about 100 events of the ultra-rare decay $K^+ \to \pi^+ \nu\overline{\nu}$ with a signal-to-background ratio of 10 in about two years of data taking at the CERN Super Proton Synchrotron [1, 2].

The NA62 beam tracker is composed of three GTK stations, installed upstream of the fiducial decay region, that provide precise momentum, angle and time measurements of the beam particles [3]. A station is composed of a 60×27 mm^2 single silicon sensor bump-bonded to ten read-out chips, each featuring 1800 $300 \times 300\,\mu$m^2 pixels.

The total beam rate is close to 1 GHz, therefore measurements of kaon rare decays with high statistics and low background demand a time-tagging resolution better than 200 ps to associate the correct parent kaon track with the decay products. Single track efficiency must be higher than 99% per single GTK station. In addition, operation in vacuum and a total material budget of less than 0.5% X_0 per station is required in order to reduce multiple scattering and hadronic interactions to acceptable levels. To cope with these stringent requirements we opted for a solution which combined a 200 µm thick silicon sensor bump bonded to 100 µm thick read-out chips thermally coupled to an ultra-thin cooling plate based on micro-channel cooling technology [4].

In addition each GTK station will have to withstand high and non-uniform hadron fluences, with a maximum in the center of about 2×10^{14} 1 MeV n_{eq}/cm^2 expected in one year of data taking in the NA62 environment. This paper presents the characterisation of non-irradiated detectors only.

2 Prototype read-out chip with time-over-threshold readout

The most challenging requirement for the GTK detector is the time resolution with such a high channel density, which can be achieved by reducing the jitter of the signal and by carefully compensating for the signal time-walk. For this purpose, a read-out architecture based on an on-pixel Time-over-Threshold (ToT) circuit followed by a time-to-digital converter (TDC) shared by a group of pixels has been designed and produced as small-scale prototype in 130 nm IBM CMOS technology [5].

Signal amplification and discrimination are performed in each pixel, and the discriminated signals are propagated to the chip periphery through dedicated transmission lines using the pre-emphasis technique in order to maintain timing precision. Processing inside the pixel cell is thus minimised to reduce noise to a minimum: hit arrival times are measured using a delay-locked loop based TDC with 98 ps bins at the end of the pixel columns. Two time measurements are performed for each hit (leading and trailing edges) and the time-over-threshold of the signal is used for offline time-walk correction. The architecture of the chip is such that these time measurements are sent out every time a hit is registered without the need of a trigger signal.

The prototype chip contains a main array of 45 pixels (a folded full column) with nine end-of-column TDC blocks each one serving five pixels through an arbiter block. In addition it includes a small array with nine pixels and a test array of six test pixels with analog output, for a total of 60 pixels. For the purpose of the test-beam, only the folded full column was read out: in this paper we focus only on the performance of the corresponding 9×5 pixel matrix ($2.7 \times 1.5\,\mathrm{mm}^2$ active area).

Five pixels are multiplexed to a single TDC channel: 9 TDCs for the leading edge time and 9 TDCs for the trailing edge time are used for each pixel column. A digital arbiter circuitry has been designed to send hit pulses to the TDC banks and block signals from the same group of 5 pixels in case they would overlap in time. These overlaps are flagged and the information is added to the output data stream.

Based on the successful prototype tests, a full scale version of the chip named TDCpix has been developed [6] and is currently being commissioned in the NA62 experiment.

3 Test-beam setup

This paper reports the results of a dedicated test-beam performed at the CERN T9 beamline (PS East Hall). A secondary hadron beam (mainly π^+ and p) with 10 GeV/c momentum, typical divergence of about 2 mrad and spot size of 1 cm, traversed four consecutive GTK detectors. The instantaneous beam intensity was kept intentionally to about 4×10^4 particles/cm^2·s, a much lower value than the one expected during NA62 operations but instrumental to reduce pile-up effects and measure detector properties in the best possible conditions. Beam particle extraction lasted 400 ms out of an overall period of several seconds.

Given the small dimensions of the active detector area, an accurate alignment with respect to the beam was needed in order to maximise the number of tracks passing through the active parts of four consecutive detectors under test (DUTs). For that reason the DUTs were installed on the precisely aligned mechanical supports shown in figure 1. Pre-alignment was achieved by installing one DUT after the other, and aligning the reference marks on the silicon sensor back-side to a precision of about 150 µm with the help of theodolites. The sensors were then protected from

2015 JINST 10 P12016

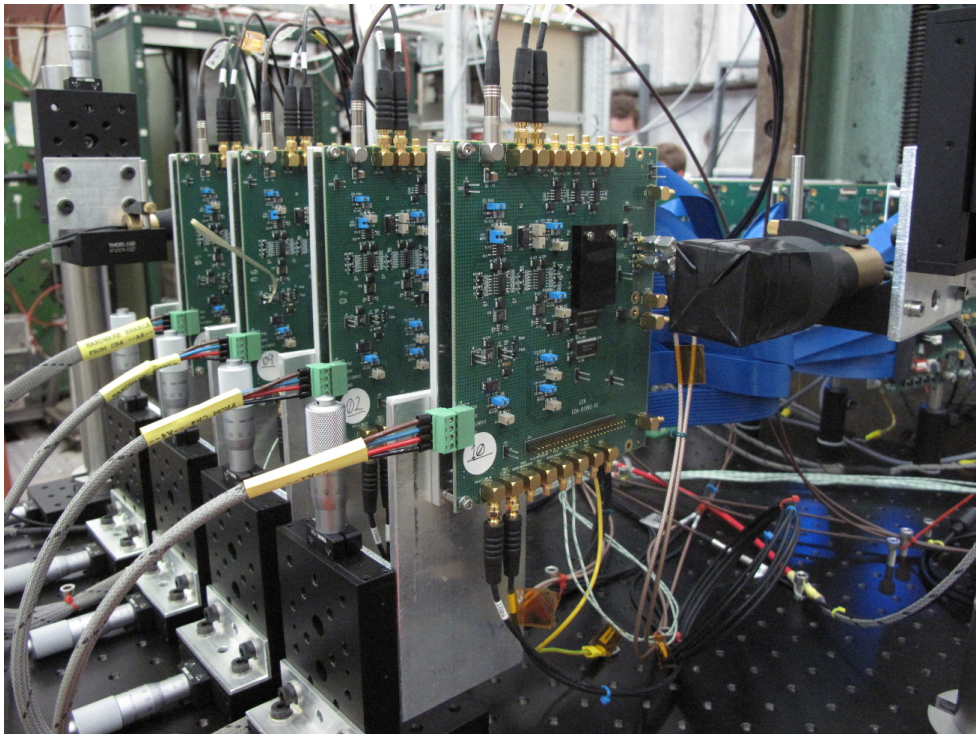

Figure 1. Picture of the four GTK detectors mounted on precisely aligned adjustable supports.

illumination by a black cover. The DUTs were connected to custom printed circuit boards (PCBs), installed on linear translational stages with 10 µm resolution for fine adjustment of the detector position perpendicularly to the beam. The distance between consecutive DUTs was 10 cm, while the detector PCBs and read-out boards were separated by 40 cm in the direction perpendicular to the beam to avoid any beam interactions with the external digital read-out electronics. A set of finger scintillators (about $3 \times 6\,\mathrm{mm}^2$) were used for alignment and monitoring and were mounted on the same optical breadboard used for the DUTs. Signals from two scintillators bars read out by four photo-multiplier tubes were combined to provide the precise time reference of a beam particle crossing with a resolution of about 50 ps (later referred to as "fast scintillators").

3.1 Detectors under test

The sensor is a planar p-in-n silicon produced by Fondazione Bruno Kessler from 200 µm thick float zone wafers. Approximately $15{\times}10^3$ e-h pairs are generated by a minimum ionising particle crossing the sensor (most probable value), corresponding to 2.4 fC. The electrical signal is propagated from the pixel through the bonding bump to the amplifier, with average gain of 65 mV/fC and a r.m.s. spread smaller than 2%.

Few tens of Volt were sufficient to completely deplete the sensor, that was operated at high over-depletion (300 V) for a large fraction of the test-beam. Bias voltages were also set to 100, 200 and 400 V on selected DUTs in order to test the system performance. DUTs were not actively cooled and were exposed to ambient temperature and humidity. No sensor breakdown was observed up to voltages slightly above 400 V.

2015 JINST 10 P12016

For the prototype read-out chip, the threshold value of the on-pixel discriminators was set by a unique digital-to-analog converter for all pixels. The thresholds during the test were set to an average value of 0.7 fC and showed a r.m.s. spread of 0.17 fC. With these thresholds, a very low level of noise was measured during the whole test-beam, as no pixel hits were recorded in the out-of-spill period.

3.2 Data acquisition system

The data acquisition (DAQ) system was formed by two independent components: one for the four DUTs and the other for the scintillators.

The first of these comprised a custom designed PCB to which the DUTs were glued and wire bonded, providing locally regulated power supplies and the necessary references. This card was designed to interface to a commercially produced FPGA evaluation board for which firmware was written to buffer and packetise the data sent from the DUTs. The data were then transmitted over Ethernet to PC for logging. The DUTs operate in a triggerless (or self-triggered) fashion, time stamping and sending all discriminator activity off-chip serially, and the readout was implemented in the same manner, packetising and sending all packets to the PC without any on-line data suppression.

The scintillators read-out was based on the CAEN V1290N TDC operated in "trigger matching mode": the TDC records all the hits in a time window which is opened each time it receives an external trigger signal. The CAEN TDC clock was provided by an external 40 MHz frequency generator, while the DUT read-out used a 320 MHz external clock, phase-locked to the previous one. To ensure synchronisation between the two read-out systems, the DUT and scintillators DAQs were correlated on a spill-by-spill basis: a common reset was issued at the start of spill after delivery of a "spill warning" signal. This signal was also connected to one CAEN TDC channel, and the pulse trailing edge gave the global time reference.

In order to cover the whole PS spill length (400 ms) without interruptions we exploited the "Extended Trigger Time Tag" feature of the V1290N. When enabled the trigger signals are time tagged, therefore we could time-stamp each hit without ambiguity by measuring the hit arrival time inside a window. For our application a window length of 51 µs was set and trigger signals were generated by a pulse generator at 20 kHz in order to have a small overlap between the windows.

4 Data analysis

Data from the two DAQ streams were logged on independent files: at the analysis stage they were reprocessed, filtered and merged to a single file format.

DUTs and scintillators data were time-aligned on a spill by spill basis. During the test beam, a slow drift of the time offsets between the scintillators and DUT DAQs was observed and corrected for prior to the analysis. This effect, of the order of nanoseconds, is mainly caused by the change of ambient temperature during the data taking period. To ease the analysis we defined an "event" by requiring scintillators coincidence together with at least one hit in one or more DUTs within a 10 ns window. Given the beam intensity and size of the active detector area, the probability of having more than one particle crossing the DUT in the event time window was negligible.

2015 JINST 10 P12016

4.1 Time walk and pixel time offsets

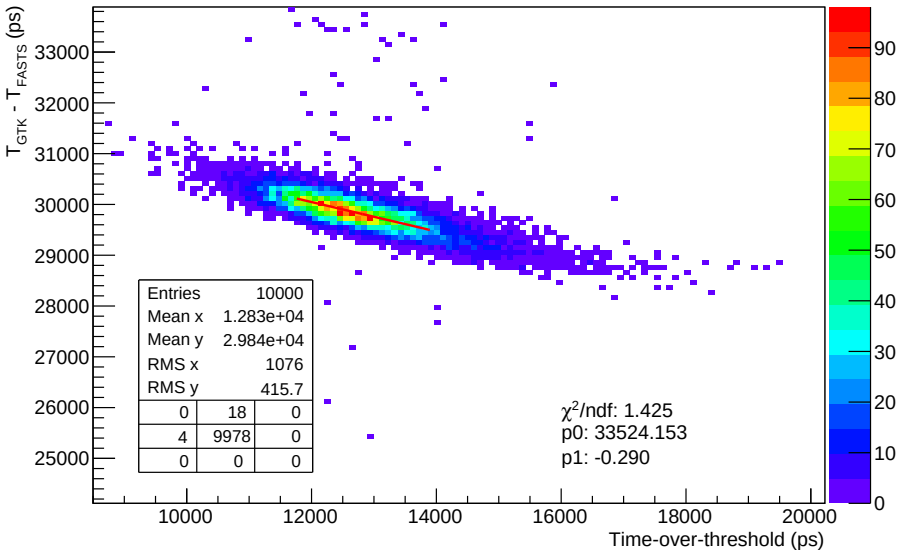

Figure 2. Distribution of time difference between a DUT pixel leading time and fast scintillators as a function of the time-over-threshold for the same pixel. A linear fit is shown, together with fitting parameters.

For a precise time determination it is mandatory to apply to each pixel the correction due to time-walk and that related to the different path length of the discriminator signal from the pixel to the TDC. With our setup both corrections can be determined by comparing the DUT hit time to the fast scintillators combined time (T_{FASTS}).

For each pixel, the time difference between DUT leading time and the fast scintillators combined time was plotted as a function of the DUT time-over-threshold, which is the difference between trailing and leading times. In figure 2 we show a plot of DUT leading time as a function of ToT for a typical pixel. For each pixel a linear fit was performed and the line parameters were combined to correct both for time-walk and offsets. An alternative correction method was applied by slicing the two-dimensional plot using 100 ps wide bins in ToT and determining the mean of $T_{\mathrm{DUT}} - T_{\mathrm{FASTS}}$ for each bin. These values were stored in look-up tables and time-walk corrections were applied for each pixel, obtaining similar time resolutions as the previous method.

In the prototype TDCpix chip used in this test-beam, when a pixel of a 5-pixel hit arbiter group is hit consecutively, the absolute delay of the second hit will be shifted in time by a constant, deterministic, time delay. In order to simplify the analysis for time resolution measurement, consecutive pixel hits belonging to the same 5-pixel hit arbiter group are rejected, resulting in a 20% loss of the available data statistics.

4.2 Clustering and tracking

An algorithm was implemented to cluster hits in adjacent pixels when they fall in a 10 ns time window. For each cluster, position and leading time are defined as the mean of the individual pixels values weighted by their respective time-over-threshold.

The DUT misalignment in the plane perpendicular to the beam was corrected by measuring residual position distributions. Tracking for the purpose of efficiency calculation was performed using three stations out of four: a line is fitted using three clusters and the extrapolated track impact point is calculated for the fourth station.

5 Detector performance

After applying the proper data quality cuts, alignments and corrections, the GTK prototype performance is evaluated in the following sections.

5.1 Time resolution

GTK time resolution was computed using two independent methods, the first relying on the time difference between two consecutive DUTs and the second computing the time difference between one DUT and the combined fast scintillator detectors.

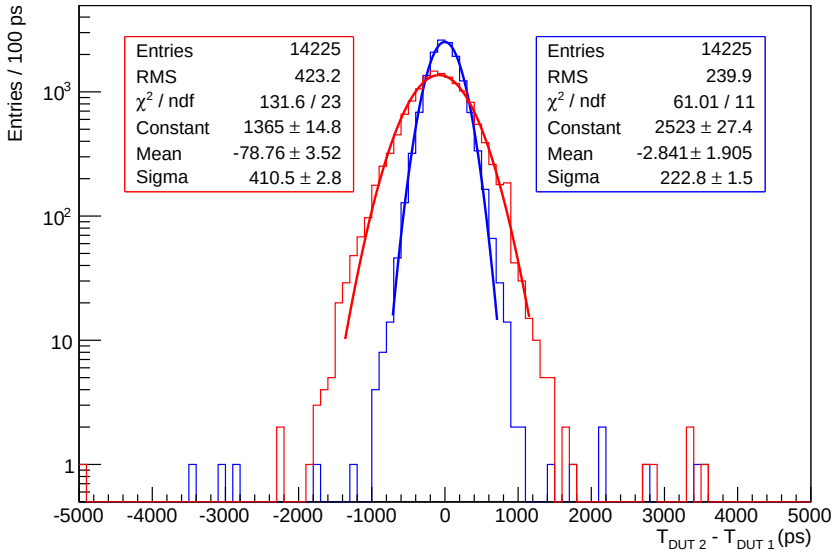

Figure 3. Distribution of the time differences between two aligned pixels for two consecutive DUTs at a bias voltage of 300 V. The red and blue curves are, respectively, before and after the time-walk and offset corrections.

The distributions of time differences between hits for the same pixel position of two consecutive DUTs, before and after time-walk and offset corrections, are shown in figure 3 for 300 V bias voltage applied to the sensor. By assuming identical resolutions we can divide the width of the distribution by $\sqrt{2}$ to extract the single pixel time resolution. Then for a single hit we obtained a time resolution of 290 ps prior and 160 ps after corrections.

The time resolutions calculated with the above method for all the 45 pixels of a typical DUT are represented by the blue dots of figure 4. Similar resolution values are obtained by making the time difference of DUT and fast scintillator detectors, as shown by the red dots in the same plot. For a bias voltage of 300 V, the time resolution for most pixels lie in a 10 ps wide band around 160 ps.

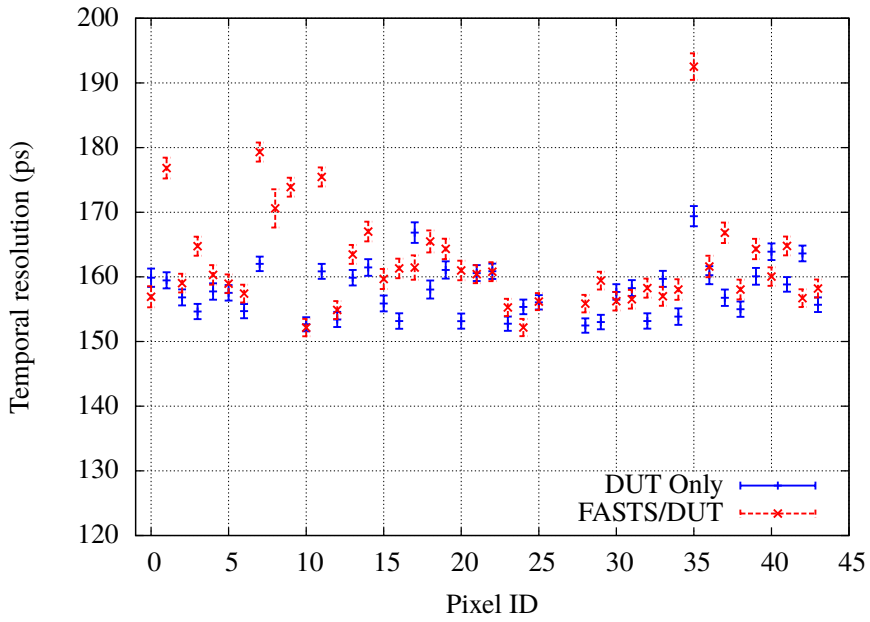

Figure 4. Time resolution distribution for all pixels of a DUT for a sensor bias voltage of 300 V. Vertical bars represent the 1-sigma error on the time resolution given by Minuit after the gaussian fit. Deviations from the mean value are observed for a few pixels, which have lower thresholds than the others.

Timing resolution computed using the fast scintillators is slightly worse due to large tails in the combined scintillators resolution and due to the non-perfect timing alignment. Large deviations from the average value are observed for few pixels and are mainly due to pixels with very low threshold (smaller than 0.45 fC). This effect becomes clear when looking at figure 5, which shows the hit time resolution as a function of the individual pixel threshold: for very low threshold values the time resolution is worse since the signal slope is smaller. It should be noted that the time-walk and offset correction depends on the pixel threshold value, therefore a new correction had to be applied to each pixel when changing the threshold value.

Time resolution dependence on the silicon sensor bias voltage is shown in figure 6, measured with data from the DUTs only and with the fast scintillators as reference, too. As expected, charge carrier velocity increases with the applied electric field up to the saturation value, which is not yet reached at 400 V. It is worth noting that the NA62 requirement on timing resolution is met at 200 V already, with a resolution better than 200 ps on single hits.

5.2 Charge sharing between pixels

While charge carriers drift through the sensor under the action of the electrical field, they diffuse laterally. For a particle impinging on the pixel at small distance from the edge, a fraction of the released charge will be collected by the adjacent pixel. To reject as much as possible clusters caused by knock-on electrons, we selected only those with two pixels and rejected events with very high energy deposition (with time-over-threshold higher than 20 ns).

The fraction of two pixels clusters over single pixels is plotted in figure 7 for different sensor bias voltages, showing a strong dependence as expected. This fraction depends also on the pixel

2015 JINST 10 P12016

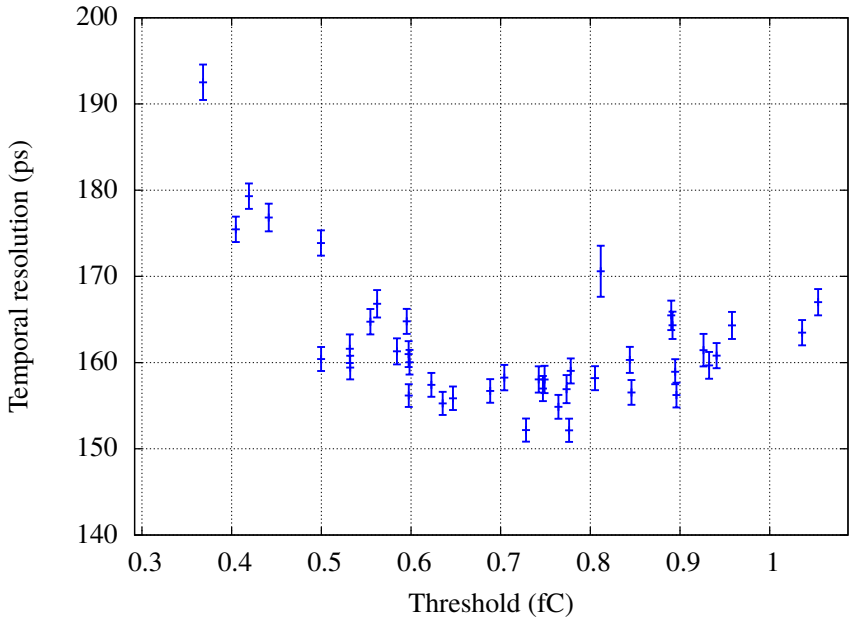

Figure 5. Time resolution as a function pixel threshold, for 300 V silicon bias and using the fast scintillators as time reference. The data points in this plot (and their errors) correspond to the red crosses of the previous figure, as they refer to the same DUT.

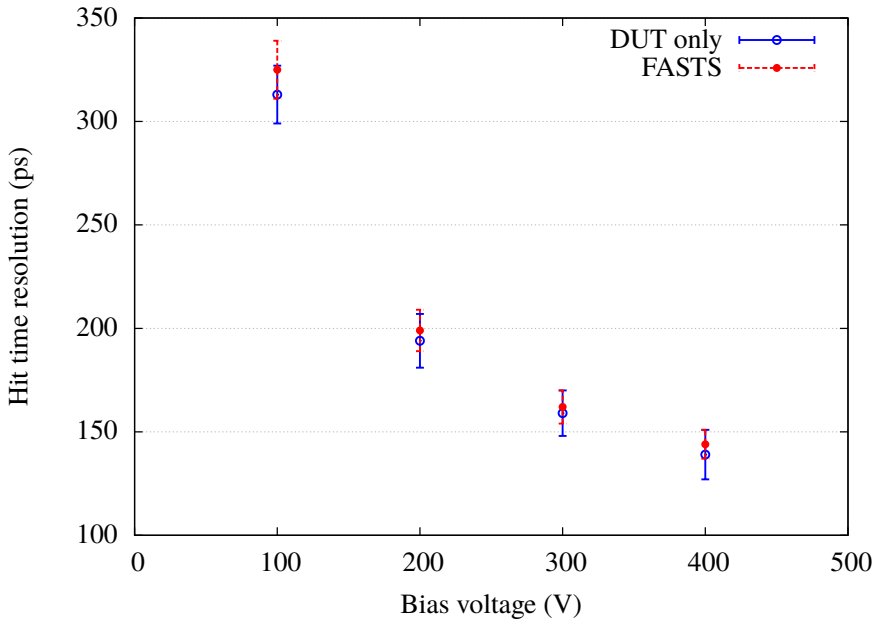

Figure 6. Time resolution as a function of sensor bias voltage for different DUTs, calculated using the two methods described in the text. Each data point refers to the average time resolution calculated for all pixels in the DUT, while the error bar represents the corresponding standard deviation.

2015 JINST 10 P12016

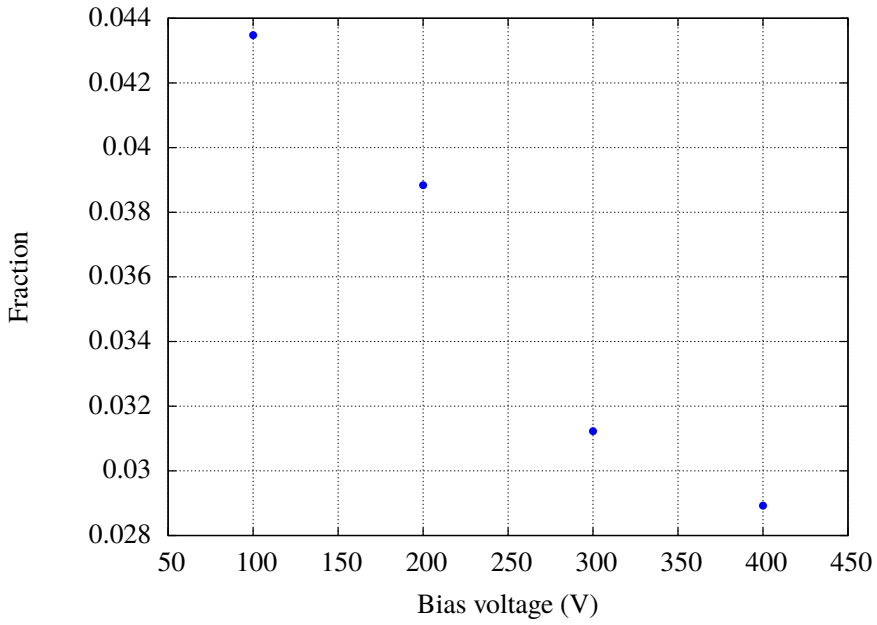

Figure 7. Fraction of two pixel clusters over single pixel clusters as a function of the bias voltage.

thresholds, and given the large number of adjacent pixel threshold combinations only the average value across all pixels is shown for a given bias (corresponding to an average threshold of 0.7 fC). For 300 V bias the charge sharing probability is 3.6% and is compatible with the value computed with a simple analytical model considering drift velocities and lateral diffusion (neglecting signal induction into adjacent pixel and capacitive coupling). This model allowed to estimate a probability of about 3% for a minimum ionising particle, impinging orthogonally and uniformly distributed over the sensor surface, to fire two adjacent pixels operated at 300 V with 0.7 fC thresholds.

5.3 Particle detection efficiency

A sub-sample of the selected events has been defined by requiring exactly one hit in each of three DUTs: the fourth target DUT is left free of constraints. A track fit is performed in both horizontal and vertical directions, and the extrapolated track impact position to the target DUT is calculated. The plot of residual positions shows a r.m.s. of about 110 µm for both views of the target DUT.

Given the relatively poor extrapolated track position resolution (due to the 300 µm wide pixels plus multiple scattering, and the absence of an external tracker with finer position resolution) the detection efficiency must necessarily be calculated by looking for hits not only at the extrapolated pixel position, but also in the 8 neighbouring ones. If a matching pixel exists in the 3×3 matrix around the extrapolated pixel, we assign an "efficiency tag" to the pixel hit; conversely if no matching exists we assign an "inefficiency tag" to the extrapolated pixel. With this method we measure a detection inefficiency smaller than 1% for the central region of a DUT as can be seen in figure 8: external and dead pixels have been excluded from the efficiency calculation.

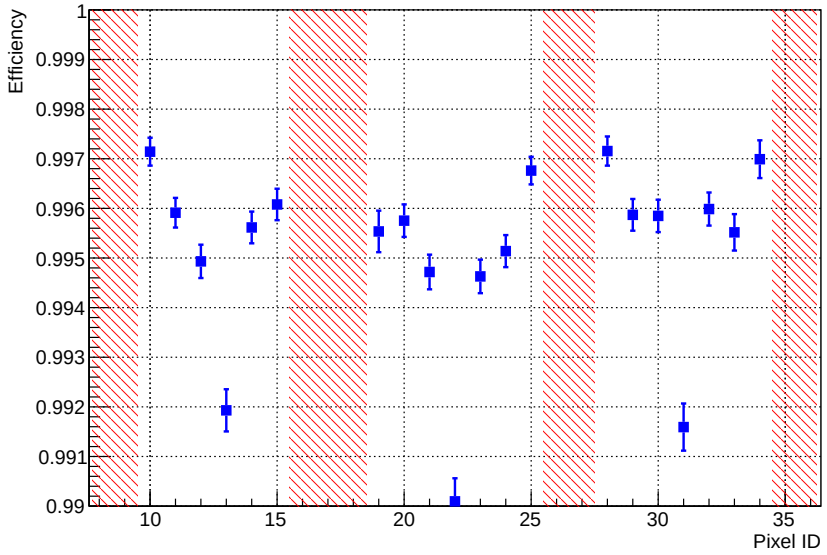

Figure 8. GTK detection efficiency as a function of pixel number. Pixels in the outer region and dead pixels have been excluded (red hatched area). The error bars refer to the boundaries for a Bayesian confidence interval assuming a binomial process.

Conclusions

The performance of the NA62 Gigatracker prototype detector has been evaluated in a dedicated test-beam using 10 GeV/c charged hadrons beam. The requirements of the experiment in terms of time resolution and efficiency are completely fulfilled; the detector shows a time resolution better than 200 ps at 200 V and a detection efficiency higher that 99%. When operating the silicon sensor at 400 V bias we measured an unprecedented resolution of less than 150 ps for a hybrid pixel detector. The clear time resolution trend with bias voltage suggests that even smaller values can be reached provided the bias voltage could be increased to reach charge carriers saturation speed.

Acknowledgments

The authors would like to express their gratitude to Crispin Williams for providing the fast scintillators used in the test-beam. Special thanks are due also to Ian McGill and Alan Honma from the CERN wire bonding team, to the CERN PS and East Area teams and to the CERN surveyors for their dedicated support and work.

References

[1] G. Anelli et al., *Proposal to measure the rare decay $K^+ \to \pi^+ \nu\bar{\nu}$ at the CERN SPS*, CERN-SPSC-P-326.

[2] NA62 collaboration, *NA62 Technical Design Document*, NA62-10-07.

[3] M. Fiorini et al., *The P326 (NA48/3) Gigatracker: Requirements and design concept*, *Nucl. Instrum. Meth.* **A 572** (2007) 290.

2015 JINST 10 P12016

[4] G. Nuessle, A. Mapelli, M. Morel, P. Petagna, G. Romagnoli and K. Howell, *NA62 GigaTracKer Cooling with Silicon Micro Channels*, in *Astroparticle, Particle, Space Physics and Detectors for Physics Applications*, Vol. 8 (2014) 525–530.

[5] P. Jarron et al., *Development of the ASICs for the NA62 pixel Gigatracker*, in proceedings of the *Topical Workshop on Electronics for Particle Physics*, Naxos, Greece, 15–19 Sep 2008, pp. 90–94, CERN-2008-008 (2008).

[6] A. Kluge, G. Aglieri Rinella, S. Bonacini, P. Jarron, J. Kaplon, M. Morel et al., *The TDCpix readout ASIC: A 75ps resolution timing front-end for the NA62 Gigatracker hybrid pixel detector*, *Nucl. Instrum. Meth.* **A 732** (2013) 511.

2015 JINST 10 P12016